

DIAMOND ULTRAVIOLET IMAGERS

M. A. Plano,¹ M. I. Landstrass,¹ S. Han², L. S. Pan², S. McWilliams¹, and D. R. Kania¹

¹Crystallume, 125 Constitution Drive, Menlo Park, CA 94025 (415) 324-9681

²Lawrence Livermore National Laboratory, L-476, 7000 East Avenue, Livermore, CA 94550

ABSTRACT

Both polycrystalline and homoepitaxial diamond ultraviolet imaging sensors have been fabricated and tested. The photoconductive detector layout consists of interdigitated metal fingers with channel lengths as small as 5 μm . The devices are fabricated by photolithography using sputtered Ti/Au contacts. The detectors exhibit high sensitivity to ultraviolet light and several of the devices exhibit gain. All of the diamond devices were tested electrically in the dark and during ultraviolet illumination from a deuterium lamp.

INTRODUCTION

Diamond's large band gap (5.45 eV) and high resistivity makes it a good candidate for use in ultraviolet detectors. Simple photoconductive devices made by fabricating ohmic contacts on the diamond surface are sensitive to wavelengths less than ~ 230 nm. By fabricating the channel on the non-encapsulated diamond surface, problems due to attenuation of the ultraviolet signal by a surface layer or dead zone are avoided. High sensitivity can be obtained with layouts such as interdigitated metal fingers which have a large active area while maintaining a channel length smaller than the recombination distance of the material. This assures total collection of the photogenerated carriers.

EXPERIMENTAL RESULTS

All diamond film growth was performed in a 2.45 GHz microwave plasma reactor facilitated with methane, carbon monoxide and hydrogen. Since impurities typically degrade the electrical properties, care was taken in cleaning the reactor and eliminating any possible sources of impurities. A variety of substrates were utilized including silicon and IIa natural diamonds (1 mm x 1 mm x 0.1 mm and 2 mm x 2 mm x 0.25 mm). Diamond samples were grown using variations in gas mixture, microwave power and substrate temperature to produce high mobility polycrystalline material on silicon (1). Homoepitaxial diamond films were grown with the

additional constraint to yield smooth single crystal films free from polycrystalline inclusions. Samples from each growth run were evaluated using Raman spectroscopy and the SEM.

As-grown diamonds were processed into surface detector devices. Figure 1 is a schematic of the interdigitated electrode configuration for the UV photoconductor. Three types of detector layouts were used, two were interdigitated metal fingers of differing pitch (5 μm for detector A and 50 μm for detector B) and the third layout, detector C, consisted of two rectangular pads separated by 125 μm . An SEM micrograph of the detector A can be seen in Fig. 2. The interdigitated layouts were patterned using photolithography. The simpler layouts were patterned using shadow masks. The metal contacts consisted of a thin Ti layer (50-500 \AA) followed by a thick Au layer (1000-5000 \AA) and were deposited by sputtering.

All of the diamond devices were tested electrically in the dark and during ultraviolet illumination from a deuterium lamp. The lamp has a broad emission from 190 nm through the visible. The power per unit area emitted in the ultraviolet range (190 nm-250 nm) was measured using a volume absorbing disc calorimeter and determined to be approximately 0.01 W/cm².

Results for the three detectors are summarized in Table I. The power listed for each device type is calculated by multiplying the lamp power density (for 190 nm-250 nm) by the device area. The current is reported for an applied voltage of 100V., both with illumination and in the dark. R is the net current divided by the power illuminating the sample and the gain is calculated by multiplying R by the energy 6.125 eV. This calculation of the gain assumes that each device has 100% quantum efficiency.

Table I. Summary of electrical results for detectors A, B, and C.

Detector type	Detector pitch	Power (W)	I total (100V.)	I dark (100V.)	I net (100V.)	R (A/W)	Gain
A poly	5 μm	3.8x10 ⁻⁶	9.0x10 ⁻⁶	1.0x10 ⁻⁹	9.0x10 ⁻⁶	2.37	14.52
B poly	50 μm	5.2x10 ⁻⁵	1.0x10 ⁻⁴	3.0x10 ⁻⁷	1.0x10 ⁻⁴	1.92	11.76
C homo	125 μm	3.1x10 ⁻⁶	1.0x10 ⁻⁴	1.0x10 ⁻⁶	9.9x10 ⁻⁵	31.94	196.0

Shown in Fig. 3 is a graph of the current versus voltage for detector A. Both the dark current and current during ultraviolet illumination is shown. The current increases by 4 orders of magnitude with ultraviolet illumination. Figure 4 is a plot of the dark current and ultraviolet current versus voltage of detector C, a homoepitaxial device. The dark current is a very low 10⁻¹³A at an electric field of 8 kV/cm., and the current during illumination is 10⁻⁵A at 8 kV/cm. The current increases by 8 orders of magnitude with ultraviolet illumination at 100V. This sample shows the largest gain, 196, of all the samples.

The speed of response of these devices was tested by measuring the conductivity as a function of time as the sample was exposed to ultraviolet radiation. The devices, both polycrystalline and homoepitaxial, took several seconds to reach a maximum current flow and several minutes to return to the pre-exposed current

levels when the light was turned off. Figure 5 is a graph of the current for an applied voltage of 10V as a function of time for detector B at three different temperatures. Both the photocurrent and the dark current increase with temperature. The activation energy of the photocurrent is 0.22 eV. It is unclear if the increase in current with temperature is due to the behavior of the deep traps or due to a contact effect with temperature. Also, the time to reach $1/e$ decreased with higher temperatures. At 300K the $1/e$ time was 17 s, while at 625K it was less than 1 s.

The diamond films used to fabricate detector B were also measured using transient photoconductivity techniques which utilize ac ultraviolet signals from a pulsed laser (2-10). A plot of the amplitude of the transient photoconductivity signal as a function of time for a natural diamond and two microwave diamond films are shown in Fig. 6. The film labeled microwave 2 corresponds to the material used in detector B. The signals generated with the picosecond pulsed laser showed a very quick rise and recovery to the ultraviolet signal. This is in contrast to the behavior of the same samples to a dc ultraviolet signal, which shows a response time of several seconds and a recovery time of several minutes. This difference in behavior is due to a smaller density of trapped charge generated with pulsed excitation.

CONCLUSIONS

Several diamond detectors were fabricated using both polycrystalline and homoepitaxial CVD diamond samples. These samples exhibited good sensitivity to ultraviolet illumination and most of the samples exhibited gain. Three types of detector layouts were used, two were interdigitated metal fingers of differing pitch (5 μm and 50 μm) and the third layout consisted of two rectangular pads separated by 125 μm . The observation of gain in these detectors is indicative of deep traps. Further evidence of the deep traps was observed in the rise and response time of the detectors to ultraviolet light. The response time of the detectors was very slow, with the time to reach $1/e$ approximately 17 seconds.

ACKNOWLEDGMENTS

This work received support from SDIO/IST, the Superconducting Super Collider Laboratory at the DOE and the Army at Fort Monmouth.

REFERENCES

1. M. A. Plano, M. I. Landstrass, L. S. Pan, S. Han, D. R. Kania, S. McWilliams and J. W. Ager, III, submitted to *Science*, December 1992, accepted February 1993.
2. L. S. Pan, D. R. Kania, S. Han, J. W. Ager III, M. I. Landstrass, O. L. Landen and P. Pianetta, *Science* 255, 830 (1992).
3. L. S. Pan, D. R. Kania, P. Pianetta, M. I. Landstrass, O. L. Landen, and L. S. Plano, Proceedings of Diamond Films '90, Sept. 1990, Crans-Montana Switzerland.
4. L. S. Pan, D. R. Kania, P. Pianetta, O. L. Landen, *Appl. Phys. Lett.* 57, 623 (1990).

5. L. S. Pan, D. R. Kania, P. Pianetta, O. L. Landen, and M. I. Landstrass, Proceedings of the Second International Conference of New Diamond Science and Technology (Mater. Res. Soc. Proc., 1991) .
6. L. S. Pan , D. R. Kania, P. Pianetta, O. L. Landen, and M. I. Landstrass in Applications of Diamond Films and Related Materials , Y. Tzeng, M. Yoshikawa, M. Murakawa, and A. Feldman eds., Elsevier, New York(1991)
7. L. S. Pan, D. R. Kania, P. Pianetta, J. W. Ager III, M. I. Landstrass, and S. Han, "Temperature Dependent Mobility in Single-Crystal and Chemical Vapor-Deposited, submitted to J. Appl. Phys.(1992)
8. M. I. Landstrass, M. A. Plano, M. A. Moreno, S. McWilliams, L. S. Pan, D. R. Kania and S. Han, Diamond Films '92/ICNDST-3, Heidelberg Sept. 1992.
9. D. R. Kania, M. I. Landstrass, M. A. Plano, L. S. Pan and S. Han, Diamond Films '92/ICNDST-3, Heidelberg Sept. 1992.
10. "Electrical Properties of High Quality Diamond Films", L. S. Pan, S. Han, D. R. Kania, M. A. Plano, M. I. Landstrass, Diamond Films '92/ICNDST-3, Heidelberg Sept. 1992.

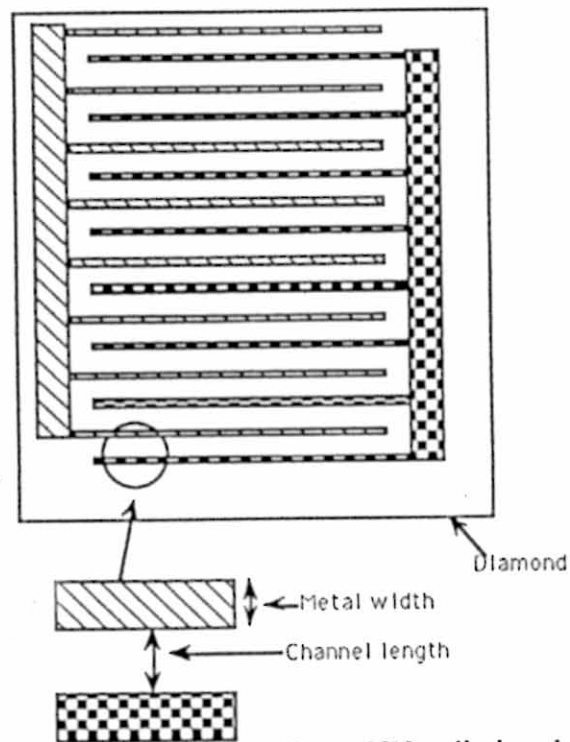


Figure 1. Schematic of the use of diamond as a UV radiation detector. Shown in the figure is an interdigitated electrode configuration for optimum collection. The device is largely defined by the finger metal width and finger channel length.

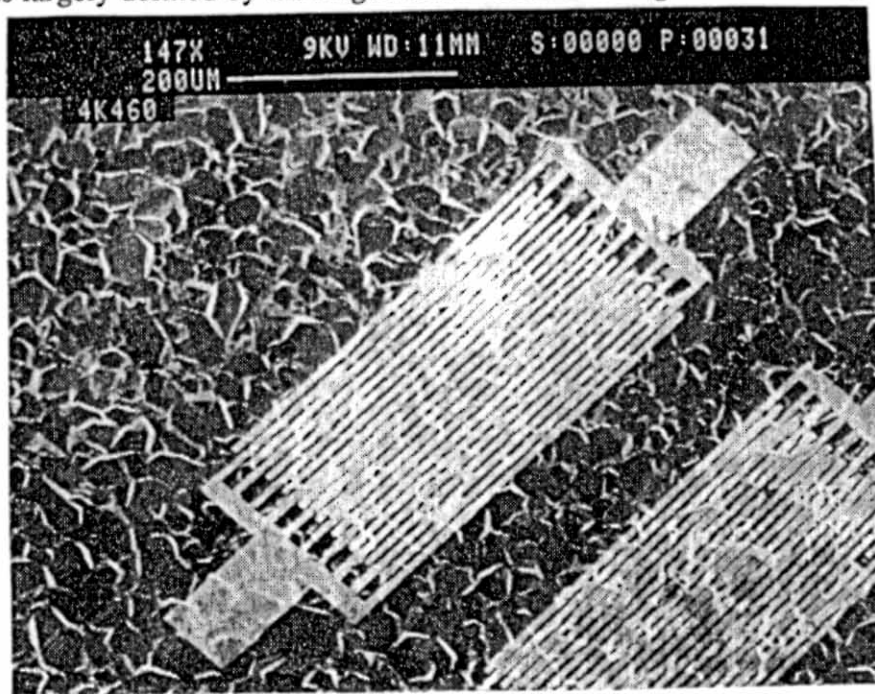


Figure 2. SEM micrograph of detector A.

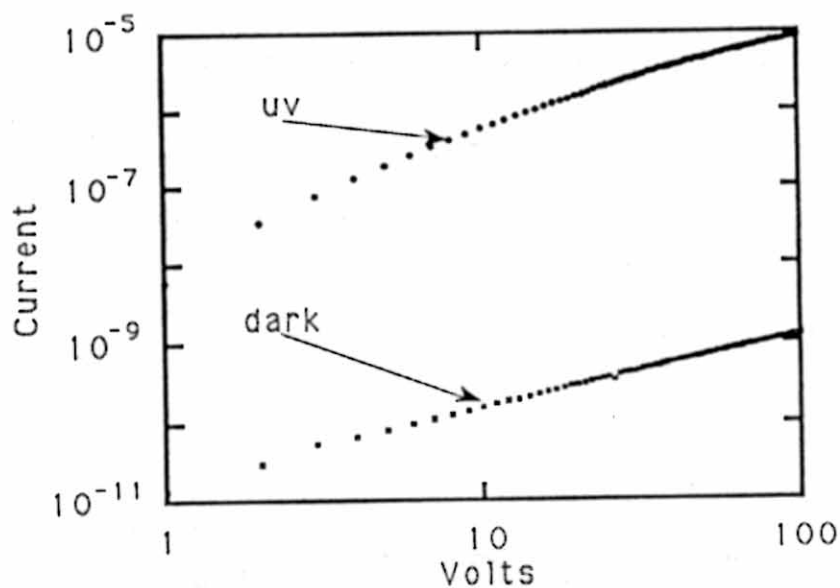


Figure 3. Graph of current versus voltage for the polycrystalline diamond detector A, both in the dark and with ultraviolet illumination.

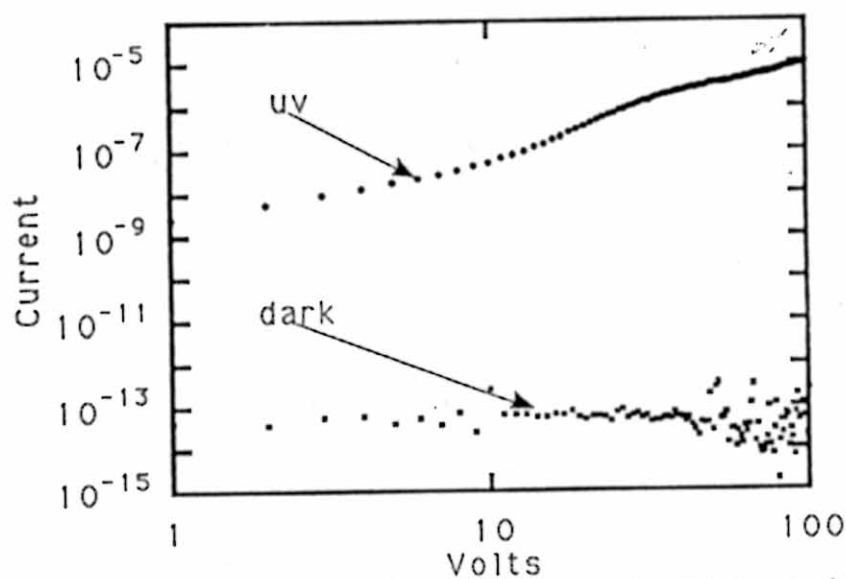


Figure 4. Graph of current versus voltage for a homoepitaxial diamond film, detector C, after annealing, both in the dark and with ultraviolet illumination.

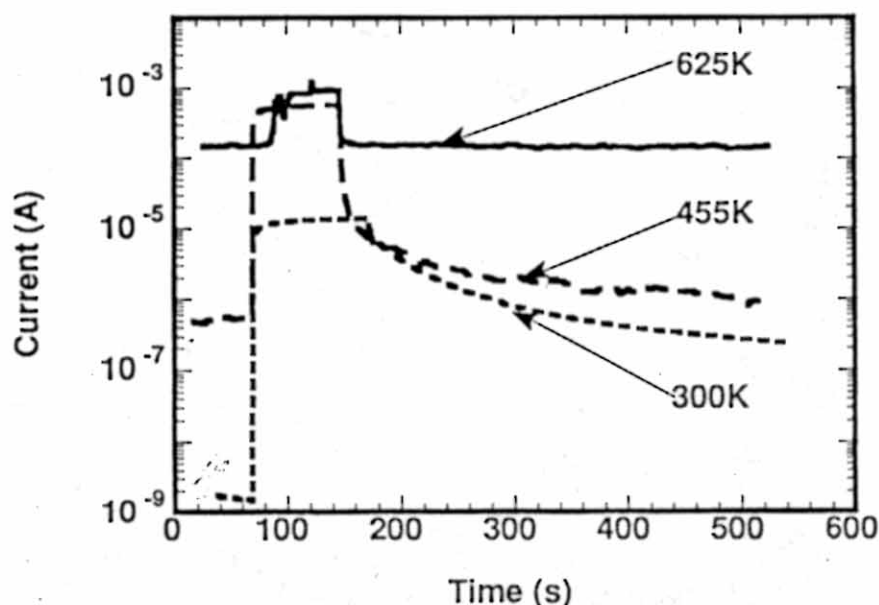


Figure 5. Graph of the current versus time of detector B as the ultraviolet illumination is turned on and off at three different temperatures. Note the increase in photoconductivity with temperature and the decrease in recovery time with higher temperatures.

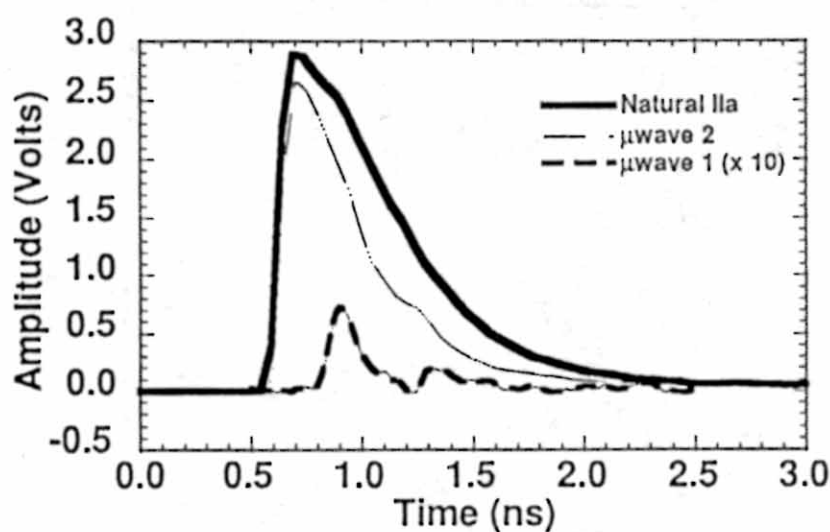


Figure 6. Photoconductive signals measured on two polycrystalline diamond films and a natural diamond. The film labeled microwave 2 corresponds to the material used in detector B.